



# Decomposition of 2-chlorophenol employing goethite as Fenton catalyst. I. Proposal of a feasible, combined reaction scheme of heterogeneous and homogeneous reactions

Guadalupe B. Ortiz de la Plata<sup>\*</sup>, Orlando M. Alfano, Alberto E. Cassano

INTEC (CONICET - Universidad Nacional del Litoral), CCT Santa Fe. Edificio INTEC I, Colectora de Ruta Nacional No. 168. Km. 472.5, 3000 Santa Fe, Argentina

## ARTICLE INFO

### Article history:

Received 17 May 2009

Received in revised form 26 November 2009

Accepted 4 December 2009

Available online 16 December 2009

### Keywords:

Heterogeneous Fenton reaction

Goethite

2-Chlorophenol

Surface reactions

Catalytic effects

Feasible reaction scheme

## ABSTRACT

A study has been conducted on the decomposition of 2-chlorophenol (2-CP) applying a heterogeneous Fenton reaction using goethite as catalyst at pH 3. The research was aimed at obtaining a workable kinetic expression apt for developing a kinetic model for scaling up purposes. Several aspects of the reaction have been described in the available literature but, for the moment, without a reasonable representation of the entire reaction behavior. In order to provide a more comprehensive and probable explanation of the whole observed performance, a set of experiments was carried out varying systematically all the significant variables. The proposal considers that the reaction is essentially a combination of four heterogeneous processes associated with one typical homogeneous Fenton reaction. Three of the surface reactions explain a very small iron leaching to the medium by a proton induced solubilization, a reductive dissolution reaction and a non-reductive iron release produced by detected 2-CP chemical decomposition byproducts, particularly, chlorohydroquinone (ClHQ) and oxalic acid (OxA). Iron concentration in the solution may be further increased in the final stages of the reaction after most of the 2-CP has been degraded, by the appearance of OxA that takes part in a third surface reaction. The fourth heterogeneous reaction rationalizes the unusual hydrogen peroxide consumption at high catalyst loadings. During the homogeneous reaction, the presence of ClHQ and ClBQ produces a homogeneous autocatalytic beneficial enhancement of the  $\text{Fe}^{3+} \rightarrow \text{Fe}^{2+}$  transformation. Consequently, the existence of phenolic derivatives either in the mixture or as reaction byproducts produces a beneficial enhancement of the reaction rate. Very low iron leaching is required to produce the onset of the homogeneous Fenton reaction, which was shown to be strongly dependent upon the reaction temperature. All the experimental findings were satisfactorily described by a set of 19-step feasible reaction scheme. The process could be useful for the treatment of wastewaters containing pollutants with phenolic derivatives, as long as iron leaching remains within tolerable limits.

© 2009 Elsevier B.V. All rights reserved.

## 1. Introduction

Environmental deterioration is a problem of increasing concern and research has been oriented to the exploration of several alternatives for pollution remediation. Among them, advanced oxidation technologies (AOTs) are receiving significant attention. The homogeneous Fenton reaction, that combines the action of hydrogen peroxide ( $\text{H}_2\text{O}_2$ ) with iron salts has been known for more than 100 years [1] and often used in many applications. It can be enhanced by increasing the temperature or application of UV-

visible radiation (the photo-Fenton reaction). These two improvements can be achieved simultaneously by employing solar irradiation. The process is usually conducted at pH 3 to maintain the iron compound in solution and requires a down-stream treatment to raise the pH and settle the catalyst. This separation is not simple for the particular colloidal characteristics of the resulting dispersion. More recently, research has been oriented to the immobilization of iron compounds on different supports to facilitate iron separation, employing mainly solid supporters to avoid more complex post-treatments [2–7]. This technology, known as heterogeneous Fenton, uses  $\text{H}_2\text{O}_2$  and employs a variety of iron immobilization techniques [7]. Alternatively, it makes use of a compact mass of iron aggregation such as different iron oxides. Several sustained compounds have been examined such as membranes [4], alginates [8], silica [9–11], zeolites [12,13], clays [14], alumina [15], glass [16,17] and activated carbon [18]. The second option includes synthesized as well as natively found iron

**Abbreviations:** 2-CP, 2-chlorophenol; ClBQ, chlorobenzoquinone; ClHQ, chlorohydroquinone; ClSQ, chlorosemiquinone; OxA, oxalic acid; PH, phenolic ring;  $M_{w-p}$ , Weisz–Prater criterion for internal diffusion.

<sup>\*</sup> Corresponding author. Tel.: +54 342 4511546; fax: +54 342 4511087.

E-mail addresses: [guadaortiz@santafe-conicet.gov.ar](mailto:guadaortiz@santafe-conicet.gov.ar), [guasaortiz@yahoo.com.ar](mailto:guasaortiz@yahoo.com.ar) (G.B. Ortiz de la Plata).

oxides [3,5,6,11,15,19–24]. Among the latter goethite seems to be a reasonable choice because it combines two attractive properties for large-scale applications: (i) wide range of operating pH and (ii) controllable leaching of iron into the solution. Other advantages have been analyzed in detail by Ortiz de la Plata et al. [7]. By choosing the optimal particle size, the catalytic activity may be maximized at the same time that the settling process can always be effective. Regarding the employed pH, even if neutral conditions appear as more favorable, is still a subject of discussion and optimization, because no definitive consensus has been arrived on the subject. This problem will be analyzed in more details below.

Some authors have considered that the reaction is just heterogeneous; i.e., the iron either acts exclusively from the solid and is permanently attached to it or in a pseudo-heterogeneous reaction adsorbs and desorbs from the surface in a continuous cycle. They have worked at pH from 6 to 9 [3,5,20,21,25–28]. A second group of studies has investigated a wider pH range from 3 to 9 [22,29,30]. With a different view, other authors have conducted the work at pH between 3 and 4 and considered that the solid compound acts as a source of very small quantities of iron that dissolves in the liquid medium and, afterwards, the process behaves as a homogeneous Fenton reaction [19,23,24]. Recent contributions with heterogeneous photo-Fenton reactions [31,32] have used pH values from 5 to 5.5. This short mention of important references is an indication that the best operating pH is still an unresolved question.

Most of these contributions to the reaction performance usually describe experimental results either addressing partial aspects of the reaction chemistry or proposing a representation of its performance with very simplified kinetics. This statement is valid for the literature reporting studies either in supported or direct use of iron oxides. In some of them, useful information has been produced concerning some specific chemical aspects of the reaction or the physicochemical properties of the iron catalyst. Noteworthy, only a few of the quoted references have proposed a possible – generally partial – mechanistic interpretation of their result. As an exception, Lin and Gurol [3] made an exhaustive proposal, but only for hydrogen peroxide decomposition in the presence of solid iron compounds. Other investigations were more interested on pollutant degradation reactions publishing useful but limited/partial reports concerning the entire reaction, such as [19,25,30,32]. Compared with Fenton and photo-Fenton studies in homogeneous systems, there is not equivalent information regarding the proposal of a complete mechanism for heterogeneous Fenton or heterogeneous photo-Fenton reactions; according to a very recent review this is also true for their applications to pollutant degradation [33]. Part of the conclusions of this review are a list of unsolved problems to indicate that much work is still needed in order to transform the Fenton family of reactions into a proven, practical process.

This work is an attempt to propose a plausible reaction scheme for a heterogeneous Fenton reaction employing goethite and, in addition, an extension to the enhancement activity of a family of chemical systems where quinone derivatives may be present or detected as intermediate reaction products. 2-CP has been chosen as model compound. The results provide supplementary and unreported quantitative insights on the reaction behavior to several already known facts of this rather complex process. Combining both sources of information it is possible to end up with a more comprehensive reaction scheme that could serve as a basis for incremental improvements. One of the important questions to answer in these cases is the possible existence of combined heterogeneous (surface and/or interfacial) and homogeneous steps (including an autocatalytic reaction path). Some of them have been qualitatively reported previously, while others have not been thoroughly elucidated or interpreted before. In addition, it seems

important to investigate the possibility that internal or external mass transfer limitations on the iron oxides interfacial reactions affect the rate since these liquid–solid interactions have been supposed to be the rate-determining steps [19]. The usefulness of this undertaking is to provide a practical proposal of the reaction performance, for a subsequent detailed kinetic study and, afterwards, the extension to enhanced operations with radiation and/or temperature. With these objectives, the effect of temperature, the ratio of  $\text{H}_2\text{O}_2$ /2-CP molar concentrations and the catalyst loading were investigated. In addition, the influence and magnitude of different forms of iron leaching into the solution and the enhancement effects of some reaction intermediates are studied.

## 2. Selection of operating conditions

For future applications, several aspects deserve an initial decision. The choice of 2-CP concentration as well as the range of molar ratios of  $\text{H}_2\text{O}_2$  with respect to 2-CP are part of a typical experimental design and does not require an extensive analysis. It is well known that this ratio has an optimal range of concentrations that must be found for every family of compounds; i.e., the only aspect that cannot be disregarded is the eventual negative effect resulting from the application of an insufficient amount or a disproportionate excess of  $\text{H}_2\text{O}_2$  concentration [33–38]. With respect to other variables, six points are worth to examine. (i) The employed particle dimensions should be the result of a compromising solution [2,3] between the largest surface area (namely, the smallest size) from the catalytic point of view on one hand, and the eventual extension to a heterogeneous photo-Fenton alternative (hindering light penetration) and the fast settling in the post-treatment on the other hand. From the data of Lu [19] and our own settling experiments, particle sizes between 75 and 150  $\mu\text{m}$  were adopted. Furthermore, we cannot disregard the negative effect that a large surface area resulting from very small particle sizes may have on the system due to the known catalyzed hydrogen peroxide decomposition by a large family of transition metal solids as it will be discussed in the next sections. (ii) Temperature is a variable that has not been quantitatively explored in detail. It may improve the decomposition rate of the pollutant but, at the same time, it may produce an even faster decay of  $\text{H}_2\text{O}_2$  which already is one of the anticipated problems of the heterogeneous process. It was decided to work in the range between 25 and 50  $^\circ\text{C}$ . This variable is important; yet, in the existing literature on heterogeneous Fenton reaction it has not been quantitatively considered an instrumental variable in the explored operating conditions. In homogeneous photo-Fenton reactions, on the contrary, it has already been found to play a very important role [39,40]. (iii) The catalyst loading also obligates a compromise between the 2-CP degradation rate and the already mentioned solid catalyzed decay of  $\text{H}_2\text{O}_2$  [2,3,30]. A range from 0.5 to 2.0  $\text{g L}^{-1}$  was selected to investigate in this study. (iv) As it was mentioned in the Introduction, the employed pH has been subjected to a wide range of variations and it is known to have a strong influence on the feasibility of the process. The fastest rates in solution and with many solid iron oxides were observed at  $3 \leq \text{pH} \leq 4$  [33]. This selection, introduces the need for acidification of the reacting medium and subsequent neutralization after treatment. However, there are at least three significant additional points to consider in making a decision on the subject. (a) Excluding the use of modified Fenton reagents, by chelating for example, attractive yields at neutral pH have not been achieved in these heterogeneous systems. (b) With a few reported exceptions, it seems that usually some iron – often only traces – leaches into the solution; then, at neutral pH it may precipitate. Finally, (c) a careful study made by Lin [2] demonstrates that the decomposition rate of  $\text{H}_2\text{O}_2$  in goethite suspensions is a strong function of the

increasing pH, affecting in this manner the viability of the process; i.e., an almost 25-fold linear increase in  $\text{H}_2\text{O}_2$  decomposition has been observed when increasing solution pH from 2 to 10. The non-productive  $\text{H}_2\text{O}_2$  consumption and the need for at least mild acidic operating conditions are some of the most important aspects to solve according to the conclusions of the review made by Pignatello et al. [33]. In fact, as already mentioned, some of the most recent studies have reported working at pH close to 5 [31,32]. For the moment, searching for a plausible and practical reaction scheme, we have adopted the most typical condition of pH 3. (v) We chose to employ perchloric acid to adjust the pH because it is known that it leads to a very low transfer of ferrous ion concentration into the solution [41]. It is clear that minimizing iron leaching should be one of the targets of the heterogeneous Fenton reaction. If small iron leaching, as well as fast reaction rates could be achieved, the only unfavorable operating condition from the economic point of view would be the need for pH adjustments. (vi) Working with phenolic compounds, the Fenton and heterogeneous Fenton processes (experimentally demonstrated in this work for the latter) render quinones as reaction intermediates. It seems important to provide additional evidence to the type of influence that these intermediate products have in the reaction, particularly if the existence of a combination of heterogeneous and, additionally, homogeneous enhancement reactions (as previously found in homogeneous systems [42]) is part of the hypothesis to investigate. Thus, some special tests must be made. In particular, several additional control experiments were needed to sustain this proposal.

### 3. Materials and methods

#### 3.1. Catalyst and model compound

Goethite –  $\alpha\text{-FeOOH}$  – (particulate, catalytic grade) and 2-CP 99%+ were provided by Aldrich.  $\text{H}_2\text{O}_2$  was supplied by Cicarelli (ACS, 30%). Finally, chlorobenzoquinone (CIBQ) 95%+ and chlorohydroquinone (ClHQ) 85%+ were also purchased from Aldrich. As discussed before, pH was adjusted with perchloric acid (ByA, ACS, 70%).

##### 3.1.1. Characteristics of the catalyst

The chosen particle size was in the range of 75–150  $\mu\text{m}$ . The measured specific surface area is  $S_g = 141 \text{ m}^2 \text{ g}^{-1}$  (BET). For a particle size of 180–500  $\mu\text{m}$ , somewhat larger than the one used in this work, Lin and Gurol [3] found a value of  $120 \text{ m}^2 \text{ g}^{-1}$ . Similarly, Gordon and Marsh [43] for an intermediate particle size (180–300  $\mu\text{m}$ ) found also a value of  $120 \text{ m}^2 \text{ g}^{-1}$ . Our measured value corresponds to elemental particles of approximately 10 nm. This is an indication that the production method of the Aldrich goethite (binding colloidal particles) renders a porous material that will

force us to analyze the possible effect of internal mass transport resistances. Additional measurements produced the following values: pore volume equal to  $0.22 \text{ cm}^3 \text{ g}^{-1}$  and average pore diameter equal to 6.1 nm (Quantachrome Autosorb). The density was  $3.4 \text{ g cm}^{-3}$ . SEM micrographs are shown in Fig. 1 (JEOL JSM-35C SEM Scanning Electron Microscope). The picture on the left (110 $\times$ ) gives an idea of the employed particle size. The much greater amplification one on the right (10,000 $\times$ ), shows a better picture of the small elementary particles of goethite used in this work. This observation is consistent with the measured specific surface area, because for  $140 \text{ m}^2 \text{ g}^{-1}$  the equivalent average particle size for this goethite sample should be about 10 nm. Lin and Gurol [3] and in more details Lin [2] reported for Aldrich goethite that: (1) the concentration of the replaceable surface hydroxyl groups was  $5 \times 10^{-4} \text{ mol g}^{-1}$  measured according to the method of Stumm [44]; (2) the surface charge and surface acidity of the goethite particles determined according to the method of Stumm [44] have the following values: the intrinsic acidity constants of the surface were  $\text{p}K_1 = 6.2$  and  $\text{p}K_2 = 9.2$  and the  $\text{pH}_{\text{zpc}}$  was equal to 7.7. With respect to XRD results, they are identical with those published by Huang and Huang [11] showing only three characteristic peaks around  $2\theta = 22, 33.5$  and  $37.5$ . Nevertheless, the XRD patterns indicate that the type of goethite provided by Aldrich for both studies has a very poor crystallinity.

#### 3.2. The reactor

The reactor is a well-stirred, cylindrical tank made of polymethyl methacrylate having provisions for: (a) temperature measurement and control to guarantee isothermal operation, (b) sampling, (c) a vigorous stirring and (d) a free surface to ensure permanent oxygen saturation.

#### 3.3. Analytical methods

2-CP and CIBQ concentrations were monitored with HPLC (Waters) equipped with a LC-18 Supelcosil reversed-phase column (Supelco). CIBQ has been clearly identified as well as ClHQ by GCMS (GC, Varian CP-3800; Mass Spectrometer Detector-Saturn 2000). Total organic carbon (TOC) was measured with a Shimadzu TOC-5000 Analyzer.  $\text{H}_2\text{O}_2$  was spectrophotometrically measured with the classical iodimetric technique and ferrous ions were also analyzed spectrophotometrically with absorbance measurements of the  $\text{Fe}^{2+}$ –phenantroline complex at 510 nm (Cary 100 Bio instrument was used for both measurements). In one test case, total dissolved iron was checked also by this method using ascorbic acid as reducing agent. Routinely, total iron content in the solution was always measured by AAS (PerkinElmer A Analyst 800). When compared, both techniques produced very close results within their respective limits of detection (maximum

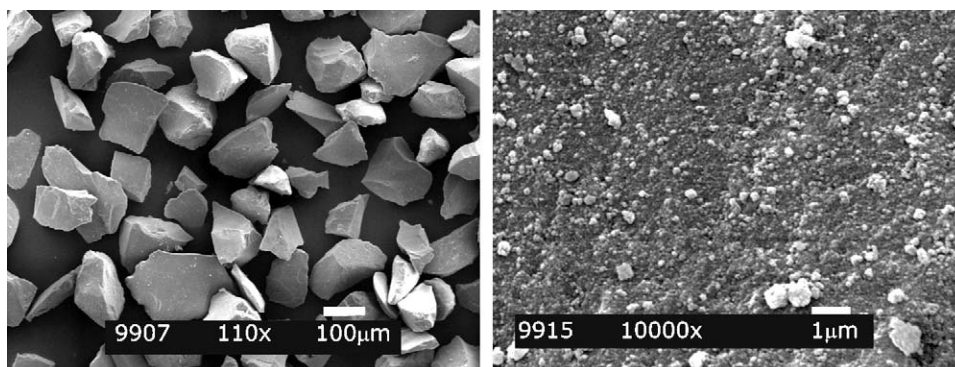


Fig. 1. SEM micrographs images of the employed catalytic goethite particles.

**Table 1**Compendium of typical experimental runs.<sup>a</sup>

Run	C <sub>Cat.</sub> ( $\times 10^{-3}$ g cm <sup>-3</sup> )	R	Temp.(°C)	X <sub>2-CP</sub> (%)	X <sub>TOC</sub> (%)	X <sub>H<sub>2</sub>O<sub>2</sub></sub> (%)	Observ.
R1T	<b>2</b>	<b>50</b>	<b>25</b>	<b>19</b>	<b>10</b>	<b>95</b>	–
R2T	<b>2</b>	<b>30</b>	<b>25</b>	<b>8</b>	<b>6</b>	<b>98</b>	–
R3T	<b>2</b>	<b>50</b>	<b>50</b>	<b>39</b>	<b>28</b>	<b>99</b>	–
R4T	<b>2</b>	<b>30</b>	<b>50</b>	<b>15</b>	<b>10</b>	<b>98</b>	–
R5T	0.5	50	25	7.3	7	47	–
R6T	0.5	30	25	6	3	53	–
R7T	0.5	30	50	98	69	99	–
R8T	<b>0.5</b>	<b>50</b>	<b>50</b>	<b>99</b>	<b>75</b>	<b>86</b>	–
R9T	0.5	10	25	2	0	55	–
R10T	2	70	25	21	12	93	–
R11T	1.25	40	25	12	9	84	–
R12T	1.25	40	25	12	9	82	–
R13T	1.25	40	37.5	48	30	98	–
R14T <sup>a</sup>	<b>0.5</b>	<b>50</b>	<b>50</b>	<b>99</b>	<b>60</b>	<b>59</b>	CIHQ(I)
R15T <sup>a</sup>	<b>0.5</b>	<b>50</b>	<b>50</b>	<b>99</b>	<b>60</b>	<b>65</b>	CIBQ
R16T	<b>0.5</b>	–	<b>50</b>	–	–	–	CIHQ(II)

CIHQ(I): initial addition of 5% chlorohydroquinone; CIBQ: initial addition of 5% chlorobenzoquinone; CIHQ(II): initial concentration of 5 ppm chlorohydroquinone.

Bold values indicate the most representative runs analyzed in Section 4.

<sup>a</sup> Results after 6 h of operation with the exception of (\*) after 3 h of operation.

difference of 10% at the lowest concentrations). Oxalic acid concentration was determined by ion-exchange chromatography using 6.0 mM NaHCO<sub>3</sub> and 4.8 mM Na<sub>2</sub>CO<sub>3</sub> as the eluent, an Ion Pack AG4A-SC column, a Waters 432 conductivity detector, and an Alltech DSPlus suppressor.

### 3.4. Operation

The reactor was filled with distilled water free of organic matter and the desired concentration of goethite was added into the solution. Then, 2-CP was added to reach the required initial concentration. After reaching steady-state temperature and confirming negligible adsorption of 2-CP, the prescribed H<sub>2</sub>O<sub>2</sub> was added into the system. pH was adjusted with perchloric acid (0.0156%, w/w). The range of the initial molar ratio of H<sub>2</sub>O<sub>2</sub>/2-CP (R) was varied from 0 to 70 (five levels) with C<sub>2-CP,0</sub> = 0.39 mM (50 mg L<sup>-1</sup>); the catalyst loading was varied in four levels from 0 to 2 g L<sup>-1</sup> and the temperature was explored in three levels from 25 to 50 °C. The initial pH was always 3.0. During the reaction it remained almost constant at values of 3.0 ± 0.1. Special runs were made adding small initial concentrations of intermediate reaction products (CIBQ and CIHQ) from the beginning of the reaction. More details on some specific control experiments will be given in the sections corresponding to results and discussion.

### 3.5. Preliminary explorations

2-CP adsorption experiments on goethite were made at pH 3 and 2-CP initial concentrations of 52.2 and 52.4 mg L<sup>-1</sup>, with the following concentrations of iron oxide: 1.5 and 30 g L<sup>-1</sup> respectively and temperature 25 °C. The latter represents a concentration 15 times larger than the largest concentration employed in this work. After 24 and 26 h for each case, the final concentrations of 2-CP were 51.8 and 51.6 mg L<sup>-1</sup>. These experiments had a RSD = 0.353% and 0.603%, respectively. Experiments with 1 g L<sup>-1</sup> at 50 °C presented similar results. The pK<sub>2-CP</sub> is 8.56 [45] and goethite pK<sub>1</sub> is 6.2. Thus, at pH 3, 2-CP will be protonated which seems to be in agreement with the observed results. Therefore, it can be concluded that adsorption of 2-CP by the catalyst was undetectable under the investigated operating conditions.

Hydrogen peroxide adsorption and reaction on the surface of goethite has been studied in details by Lin and Gurol [3]. The high instability of adsorbed hydrogen peroxide in the presence of small particles of goethite will be discussed later.

Additional test runs did not show 2-CP degradation working either with the catalyst or with the H<sub>2</sub>O<sub>2</sub> alone. Similarly, thermal,

non-catalyzed degradation was null at least up to 50 °C. The reproducibility of the experimental data of 2-CP degradation was tested under conditions where reaction intermediates could be accurately measured (see for example in Table 1, R11T and R12T).

## 4. Results and discussion

### 4.1. Salient characteristics of the reaction (Runs R3T and R8T)

Figs. 2(a) and (b), and 3(a) and (b) show results of two typical runs. The first (corresponding to R8T) describes experimental results that were made employing a catalyst loading of 0.5 g L<sup>-1</sup> and an initial molar ratio of R = 50, for an initial concentration of 2-CP = 50 mg L<sup>-1</sup> and 50 °C. In Fig. 2(a) and (b), concentration changes as a function of time are shown for 2-CP, H<sub>2</sub>O<sub>2</sub>, total iron in solution, CIBQ and TOC. CIHQ variation concentrations were not distinctly detected by HPLC as it was the case with CIBQ and are not shown in the plot (see Section 3.3, concerning GCMS analysis). The following observations can be made: (i) Both the 2-CP and the TOC concentrations show an initial induction period with a slow

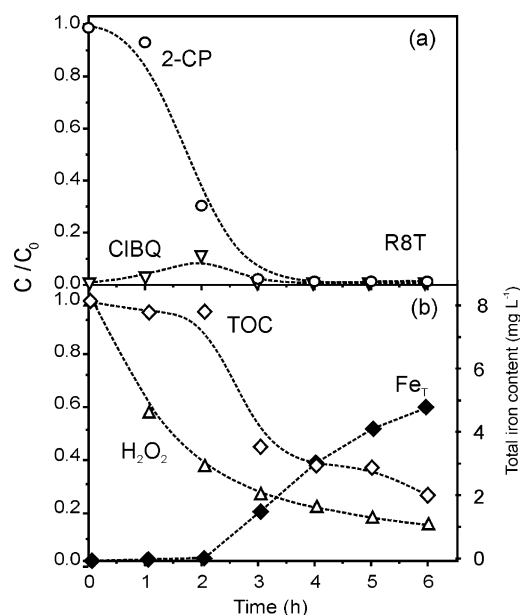


**Fig. 2.** Dimensionless concentrations of reactants and products versus time. R8T: C<sub>Cat.</sub> = 0.5 g L<sup>-1</sup>, R = 50 and T = 50 °C. (a) ○, C<sub>2-CP</sub>/C<sub>2-CP,0</sub>; ▽, C<sub>CIBQ</sub>/C<sub>2-CP,0</sub>. (b) ◇, TOC/TOC<sub>0</sub>; △, C<sub>H<sub>2</sub>O<sub>2</sub></sub>/C<sub>H<sub>2</sub>O<sub>2,0</sub></sub>; ◆, total dissolved iron.



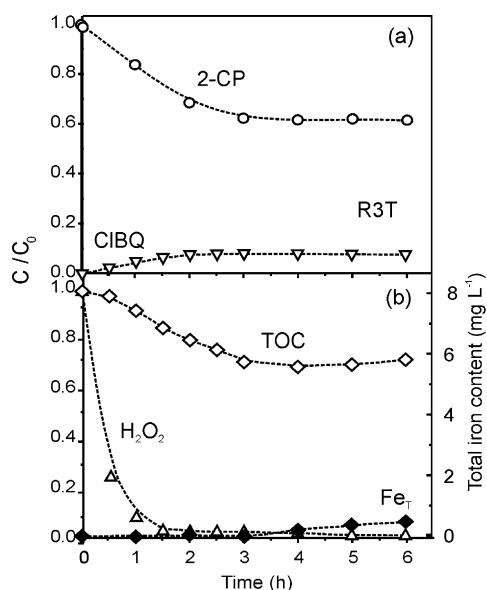


**Fig. 3.** Dimensionless concentrations of reactants and products versus time. R3T:  $C_{Cat} = 2 \text{ g L}^{-1}$ ,  $R = 50$  and  $T = 50^\circ \text{C}$ . (a)  $\circ$ ,  $C_{2-CP}/C_{2-CP,0}$ ;  $\nabla$ ,  $C_{CIBQ}/C_{2-CP,0}$ . (b)  $\diamond$ ,  $TOC/C_{2-CP,0}$ ;  $\triangle$ ,  $C_{H_2O_2}/C_{H_2O_2,0}$ ;  $\blacklozenge$ , total dissolved iron.

reaction rate. (ii) The TOC concentration change is different from the corresponding 2-CP concentration. (iii) Changes in CIBQ and CIHQ (this one, only detected by GCMS) concentrations only explain part of this difference, indicating the possible existence of additional reaction intermediates. (iv) After approximately 2–3 h of reaction time the concentration of iron raised in a steadily manner to a value of  $4.3 \text{ mg L}^{-1}$ . (v) After approximately 3–4 h, depending on the experiment, oxalic acid was detected (just for runs with complete degradation of aromatic compounds) with a maximum value of  $0.09 \text{ mM}$ . This phenomenon would explain the continuation of iron dissolution. Very low concentrations of other reaction intermediates were also observed but they were neither positively identified nor quantified. (vi) Concerning the solubilization of iron, as it will be discussed below, when concentrations are clearly above the detection limit, it can be concluded that, as long as there is some 2-CP in the medium, most of the iron present in the solution is in the form of  $Fe^{2+}$ . Afterwards, iron changed to the  $Fe^{3+}$  oxidation state. (vii) The increase in the iron concentration almost coincides with a significant enhancement of the 2-CP decomposition rate indicating the existence of an important influence produced not only by the presence of iron in the solution, but also as a possible consequence of the appearance of other effective reaction byproducts that can participate in the reaction in different ways. This point will be discussed in detail with the presentation of all the experimental results. (viii) The concentration of 2-CP almost falls to zero after 4.5 h of reaction time (99+ conversion with an iron concentration of approximately  $3.2 \text{ mg L}^{-1}$ ). (ix) The  $H_2O_2$  consumption is very significant (recall that  $R = 50$ ). (x) CIBQ and CIHQ can be detected as the main reaction intermediates during most of the reaction. Besides, after some time, particularly when the concentration of 2-CP was almost depleted, oxalic acid was also detected. Finally, (xi) once the concentration of iron in the solution increases and the concentrations of quinones become substantial in the solution, the conversion of 2-CP reaches 98.5% at a fast rate in less than 4 h. The iron concentration at this time, is approximately equal to  $3 \text{ mg L}^{-1}$ .

Results shown in Fig. 3(a) and (b) were obtained by employing a catalyst loading of  $2.0 \text{ g L}^{-1}$ : all other operating conditions were maintained as reported for Fig. 2. (i) Results in Fig. 3(a) seem to be, at first glance, contradictory if one considers that the temperature

effects in the homogeneous Fenton reaction is very significant [40]. (ii) The concentration of  $H_2O_2$  almost drops to zero shortly after 2.5 h of reaction. (iii) Under this condition, not only the 2-CP conversion is very poor but also TOC concentration follows the same pattern. Differing from Fig. 2(b), the TOC concentration has almost the same value than that the one of 2-CP which could be an indication of a diminution in the formation of low molecular weight reaction intermediates. (iii) This corroborates that the absence of  $H_2O_2$  not only stops the main reaction, but also inhibits the increase in concentration of some important intermediates. (iv) In accordance with point (iii), the iron concentration in solution reaches very small values as compared with R8T. (v) Notwithstanding the above observation, from experiments R8T and R3T it becomes obvious that once very small amounts of iron ions are present in the solution (even below the detection limits of the employed analytical methods) the degradation of 2-CP can take place at measurable rates. (vi) It is apparent that the presence of high concentration of goethite catalyzes a very fast decomposition of  $H_2O_2$  which is a well-known effect resulting from its typical degradation by some transition metals and considering the high specific surface area of the catalyst (recall that the employed goethite has a value of  $S_g = 141 \text{ m}^2 \text{ g}^{-1}$ ). This particular outcome could be in part responsible for these very different observed results. For the decomposition reaction of hydrogen peroxide with goethite at pH 7, Lin and Gurol [3] determined an activation energy of  $32.8 \text{ kJ mol}^{-1}$ , which in addition, indicates the existence of a rather moderate contribution of temperature effects in the observed results. This value will certainly be larger at lower pH values [2]. Finally, (vii) the CIBQ concentration remains almost constant. Apparently, due to the lack of  $H_2O_2$ , the degradation rate of CIBQ also diminishes. This observation must be analyzed jointly with points (ii) to (vii). The fate of  $H_2O_2$  in this reaction, even in the absence of 2-CP, will be also discussed later.

#### 4.2. Initial annotations of some of the main aspects of the reaction

From the experimental observations described in the previous introductory description of the reaction there are at least six points to analyze and to be explained in detail:

1. During the initial reaction time, we observed some sort of delayed establishment of the heterogeneous Fenton oxidation mechanism. It is an indication that the building-up of a sufficient concentration of hydroxyl radicals from hydrogen peroxide decomposition, is not facilitated promptly by the presence of enough available iron in the reacting system. In other words, in the case under discussion, the initial reaction of hydrogen peroxide with solid goethite alone does not seem to produce an appreciable amount of efficacious  $HO^\bullet$  radicals that would significantly contribute to the pollutant degradation. They may be formed on the goethite surface at an important rate, but are immediately recombined or scavenged before becoming available to oxidize 2-CP. Similar behavior has been investigated in details by Huang and Huang [11] with the same conclusions. Besides Kwan and Voelker [46] have discussed specifically the circumstance that in the Fenton reaction the consumption of  $H_2O_2$  does not equal the generation rate of hydroxyl radicals because hydrogen peroxide can be additionally decomposed to water and oxygen via non-radical producing pathways by iron oxides. In their study concerning the  $OH^\bullet$  production by iron oxides and  $H_2O_2$ , part of their conclusions imply that some reactants present in the system are either interfering the production or consuming these radicals before they can act efficiently in the oxidation of a given compound. Thus, some additional reaction step (or steps) may be necessary to explain the subsequent behavior.

- The observed induction period could indicate the existence of an initial slow transfer of iron from the goethite surface into the solution. Once it is produced, in presence of  $\text{H}_2\text{O}_2$ , the reaction rate is dramatically increased. The possibility of mass transfer limitations in the iron dissolution either due to internal diffusion inside the pores of the catalyst or at the external boundary layer of the interface liquid solution–solid catalyst, as well as their effects on the inefficient use of the  $\text{OH}^\bullet$  generated by the surface degradation of  $\text{H}_2\text{O}_2$  will be analyzed later.
- From points 1 and 2, it seems that under the adopted operating conditions, additional important contributions to the reaction path are necessary. They should put into action the solid catalyst of the heterogeneous Fenton process, in order to stimulate its function as a supplier of active iron species in the homogeneous solution; i.e., apparently, to convert the reaction into a typical homogeneous Fenton process, an unfortunately rather slow, but essential and prior mechanism is necessary. This could be explained by a sluggish surface reaction or a mass transfer limitation from the solid to the liquid phase and/or vice versa. This phenomenon, indispensable for the effective initiation of the degradation reaction, is perhaps one of the crucial mechanistic aspects that should be disclosed in details. Additionally, to unfold the existing decisive difference with those reports that consider that the process acts in a cycle where the iron never is released from the solid [3,5,20].
- Once there is enough iron in the solution (but not necessarily larger than  $1 \text{ mg L}^{-1}$ ) CIBQ not only can be detected, but its concentration also increases even further due to the following reactions: (i) The 2-CP degradation rate increases. (ii) The iron leaching rate into the solution if further promoted by the activity of reaction byproducts. The mechanism is also part of what should be unveiled as completely as possible (recall that in these instances, the presence of CIBQ was detected by employing GCMS analysis).
- Always there is an unusual consumption of  $\text{H}_2\text{O}_2$ . As shown in Fig. 3(a) and (b), in some cases, with high catalyst loadings, it could lead to a significant reduction and finally stop of the 2-CP degradation after all the  $\text{H}_2\text{O}_2$  decomposed.
- Some of the involved processes in the 2-CP degradation are almost surely affected by two important reaction parameters: (a) concentration of solids and (b) temperature. In previous studies employing solid iron oxides, some of these aspects, particularly the temperature effects, have not been quantitatively investigated so far.

In what follows, a systematic presentation of the different performed experiments will be described and discussed in detail. For reasons of better communication and discussion of the observed result, the presentation neither will follow the order of these preliminary six points nor will treat them separately due to the most likely existence of interrelationships among them.

#### 4.3. Detailed analysis and interpretation of the experimental results

##### 4.3.1. Effect of catalyst concentration and temperature

Besides the results shown previously, Fig. 4(a) and (b) for  $R = 50$  and Fig. 5(a) and (b) for  $R = 30$ , as well as Table 1, present some of the most noticeable aspects to discuss. Low temperature and very high catalyst concentration (Fig. 4(a)) are not a favorable operating condition because both the conversions of 2-CP and TOC are rather small (Run R1T) and, on the contrary, the  $\text{H}_2\text{O}_2$  consumption is very large. However, as shown in Fig. 4(b) different results are obtained with low catalyst concentration and the same temperature (Run R5T). Under these conditions, the conversion of 2-CP remains low and the hydrogen peroxide consumption is significantly smaller than in the case of Fig. 4(a). This is a confirmation of the already

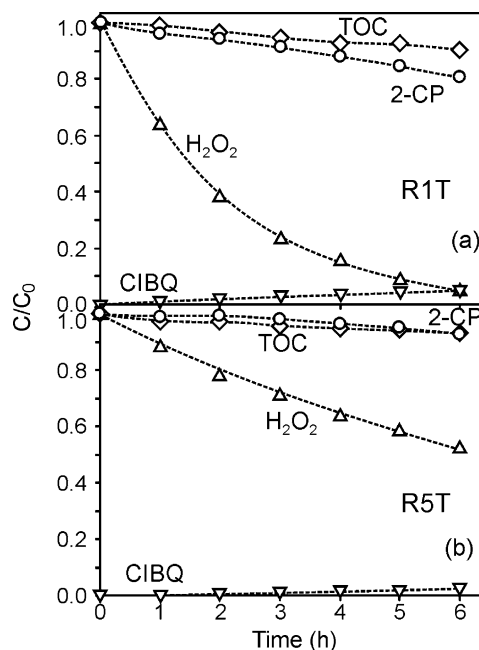


**Fig. 4.** Dimensionless concentrations of reactants and products versus time. (a) R1T:  $C_{\text{cat}} = 2 \text{ g L}^{-1}$ ,  $R = 50$  and  $T = 25^\circ \text{C}$  and (b) R5T:  $C_{\text{cat}} = 0.5 \text{ g L}^{-1}$ ,  $R = 50$  and  $T = 25^\circ \text{C}$ .  $\circ$ ,  $C_{2\text{-CP}}/C_{2\text{-CP},0}$ ;  $\nabla$ ,  $C_{\text{CIBQ}}/C_{2\text{-CP},0}$ ;  $\diamond$ ,  $\text{TOC}/\text{TOC}_0$ ;  $\triangle$ ,  $C_{\text{H}_2\text{O}_2}/C_{\text{H}_2\text{O}_2,0}$ .

mentioned high surface area and temperature dependences on  $\text{H}_2\text{O}_2$  catalyzed decomposition by some solids [3,47]. The results shown in Fig. 5(a) and (b) correspond to a similar comparison employing a catalyst loading of 2 and  $0.5 \text{ g L}^{-1}$ , but now the temperature is  $50^\circ \text{C}$ . On Run R4T, making use of a catalyst concentration of  $2 \text{ g L}^{-1}$ , it can be seen that earlier than 2.5 h of reaction, the concentration of hydrogen peroxide is not detectable and the decomposition reaction of 2-CP ceases. It can also be seen that at  $T = 50^\circ \text{C}$  the iron concentration in solution is visible but very low. These results could have a dependence on the initial molar ratio of hydrogen peroxide to 2-CP ( $R = C_{\text{H}_2\text{O}_2,0}/C_{2\text{-CP},0}$ ), but

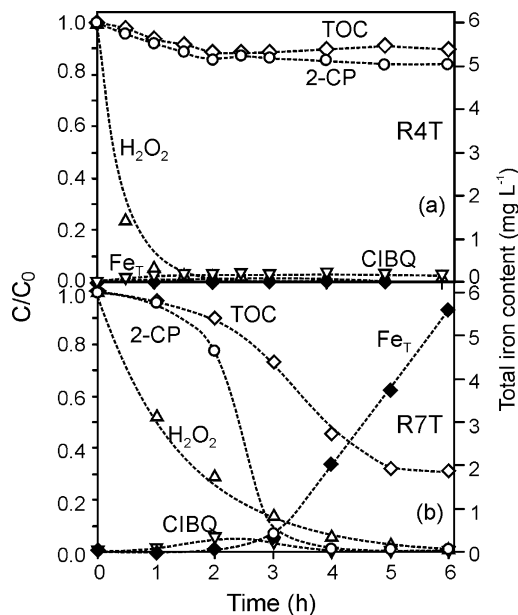


**Fig. 5.** Dimensionless concentrations of reactants and products versus time. (a) R4T:  $C_{\text{cat}} = 2 \text{ g L}^{-1}$ ,  $R = 30$  and  $T = 50^\circ \text{C}$  and (b) R7T:  $C_{\text{cat}} = 0.5 \text{ g L}^{-1}$ ,  $R = 30$  and  $T = 50^\circ \text{C}$ .  $\circ$ ,  $C_{2\text{-CP}}/C_{2\text{-CP},0}$ ;  $\nabla$ ,  $C_{\text{CIBQ}}/C_{2\text{-CP},0}$ ;  $\diamond$ ,  $\text{TOC}/\text{TOC}_0$ ;  $\triangle$ ,  $C_{\text{H}_2\text{O}_2}/C_{\text{H}_2\text{O}_2,0}$ ;  $\blacklozenge$ , total dissolved iron.

it will be seen in what follows that the optimum range for  $R$  lies between 30 and 50. This is the first heterogeneous process (a surface reaction) that has an active influence on the reaction efficiency. When the catalyst loading is smaller in R7T ( $0.5 \text{ g L}^{-1}$ ), differences are very significant: not only the 2-CP conversion is much larger at high temperature (almost 99% after 4 h with an iron concentration not larger than  $2.1 \text{ mg L}^{-1}$  at that time) but TOC conversion results also show an important increase as well (69%, Table 1). Consistently, at  $50^\circ\text{C}$ ,  $\text{H}_2\text{O}_2$  decomposition still shows high values (99%). Consequently, low catalyst concentration and high temperature are important for a good degradation of 2-CP and a reasonable degree of mineralization. The effect of increasing temperature is conclusively shown in going from  $25$  to  $50^\circ\text{C}$ , by comparing previous values with runs made at  $25^\circ\text{C}$  (R6T, Table 1) where the decomposition of  $\text{H}_2\text{O}_2$  is lower (53%), but coupled with too low 2-CP conversions. This quantitative information about this very important effect of temperature influence in heterogeneous Fenton reactions has not received very much attention in the past. Besides, at high catalyst loadings, the contrast with the performance of the typical Fenton reaction is even more remarkable. It has been effectively shown by [40] that an increase in temperature from  $25$  to  $55^\circ\text{C}$  diminishes the effect of the photo-enhancement of the Fenton reaction (from more than 150% to less than 12% relative increment, respectively). In homogeneous systems, this constitutes undoubted evidence that some of the dark Fenton reactions have a rather high activation energy that promotes this important beneficial effect of temperature, but is significantly disguised when the concentration of the solid catalyst is high.

More information can be obtained by analyzing these results with those already shown in Figs. 2 and 3. It can be definitely seen that in the first case (Fig. 2(b)) with low catalyst loading, after 6 h of reaction, there still is  $\text{H}_2\text{O}_2$  present. Conversely, in the second case (Fig. 3(b)) and even more impressive in Fig. 5(a), before 3 h of reaction, the  $\text{H}_2\text{O}_2$  concentration is almost undetectable (conversion of 99%+). Always, regardless the outcome with respect to 2-CP conversion, high temperature and, particularly high catalyst concentration, lead to an almost total decomposition of  $\text{H}_2\text{O}_2$ . In some occasions, this phenomenon takes place in a rather short time with respect to the programmed length of the experimental run (R3T and R4T). In Run R7T (Fig. 5(b)) it is possible to see that after 5 h, the iron content is below  $4 \text{ mg L}^{-1}$ ; at that point, the conversion of 2-CP is 99%+ and the TOC conversion is reaching a plateau, coinciding with the very low values of  $\text{H}_2\text{O}_2$  concentration.

Upon comparison of the results of Runs R7T and R8T (Fig. 2(a) and (b)), within limits, it could have been concluded that the value of  $R$  does not represent a very influential variable. This is not actually true. It can be seen that between  $R = 30$  and  $R = 50$  (Runs R7T and R8T) seems to be taking place the best initial concentration ratio ( $R = C_{\text{H}_2\text{O}_2,0}/C_{2\text{-CP},0}$ ). However, results not plotted here, indicate that for both catalyst loadings ( $0.5$  and  $2 \text{ g L}^{-1}$ ) when  $R$  is increased from 10 to 30 the reaction rate significantly increases; but once  $R$  attains the value of 50, the 2-CP conversion reaches a plateau and no further improvement is obtained.

#### 4.3.2. Unusual hydrogen peroxide consumption

The fast decomposition of hydrogen peroxide in the heterogeneous Fenton process is a serious problem. Moreover, we must emphasize the evidence that its presence in the reaction is essential, as it is shown in Figs. 3(b) and 5(a). This result shows the main reason of the much better performance of the lower catalyst concentration at the same temperature. However, results also show that the significantly fast rate of disappearance of  $\text{H}_2\text{O}_2$  has no correlation with a possible stoichiometric demand from the decomposition of 2-CP. In a recent work, Teel et al. [47] carried out a systematic study of the decomposition of  $\text{H}_2\text{O}_2$  catalyzed by seven different trace

minerals and four iron and manganese oxides. At pH 3, pyrolusite, goethite and hematite exhibited the fastest rates that were proportional to the surface area of the solids.

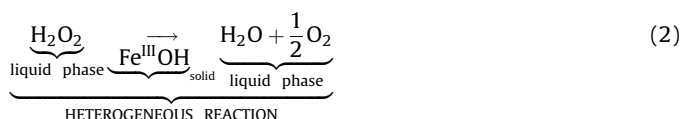
As it will be seen later when discussing mass transfer problems concerning some of the surface reactions employing porous catalysts, the  $\text{OH}^\bullet$  generated during this reaction cannot have an important effect in the process, ratifying the adverse problem associated with the ineffective destruction of hydrogen peroxide.

This reaction, employing goethite of similar characteristics than the one used in this work ( $S_g = 120 \text{ m}^2 \text{ g}^{-1}$ ) has been modeled in details by Lin [2] and Lin and Gurol [3] with a 10 steps mechanism. Resorting to conventional kinetic modeling approximations, the authors end up with a modified Langmuir–Hinshelwood model that was finally reduced to a second order reaction of the form:

$$R = -k C_{\text{H}_2\text{O}_2} C_{\text{Fe}^{\text{III}}\text{OH}} \quad (1)$$

$\triangleright$  represents bond to the matrix of the oxihydroxide surface.

With the global reaction:



At pH 7, the proposed mechanism assumes that the iron is always attached to the solid and the active site is constantly regenerated for a new hydrogen peroxide decomposition. It should be noted that by employing a constant catalyst concentration in every run, Eq. (1) indicates a first order kinetics with respect to hydrogen peroxide concentration. This first order kinetics has been plotted with the typical exponential decay in Fig. 4(a) for Run R1T and Fig. 5(b) for Run R7T in two experiments where the hydrogen peroxide decay is clearly observed.

At lower pH values as the one used in their work (from pH 10 to 4 [2]), this reaction follows a similar trend, even if it occurs with a small release of iron into the solution. It becomes clear that the catalytic action of goethite in the heterogeneous Fenton reaction encounters a highly undesired competing reaction leading to the rapid disappearance of  $\text{H}_2\text{O}_2$ . This type of process has been called by Pignatello et al. [33] the “unproductive destruction of the reactant”.

This hydrogen peroxide solid catalyzed decomposition reaction is not directly involved in the mechanism of 2-CP degradation. In fact, within the context of the heterogeneous Fenton degradation, the hydrogen peroxide consumption does not bear any stoichiometric relationship with the observed 2-CP reaction evolution. This statement is in full accordance with the comparison made of the observed reaction rates of hydrogen peroxide decomposition produced by small amounts of dissolved iron compounds by Pignatello [48] and by low concentrations of small ( $0.1$ – $80 \mu\text{m}$ ) particles of goethite (under conditions of a reported undissolved iron) by Lin [2]. The second author found three orders of magnitude faster  $\text{H}_2\text{O}_2$  decomposition rates. Similar studies have also been reported by Burbano et al. [38] in homogeneous Fenton reactions. In this work, the authors found the existence of an optimum hydrogen peroxide concentration. It is directly related to the negative consequences produced by an excess of hydrogen peroxide in a homogeneous Fenton reaction, because it enhances the effects of other reactions that scavenge  $\text{OH}^\bullet$  radicals. Recapitulating, in our work, this is an evidence of the existence of a heterogeneous surface reaction that has a strong negative incidence in the global output results in spite of the fact that presence of  $\text{H}_2\text{O}_2$  in the solution is indispensable. However, as indicated before, these effects in either heterogeneous or homogeneous Fenton reactions are not a novelty and have been also observed in previous contributions [34–36].

#### 4.3.3. Effect of the iron concentration in the solution

Either at 25 °C or at 50 °C, employing 2 g L<sup>-1</sup> of catalyst (Table 1: R1T, with the iron content too small to be plotted in Fig. 4(a), and R3T with Fig. 3(b)) the concentration of iron in the solution never reaches values larger than 0.5 mg L<sup>-1</sup>. Similarly, with 0.5 g L<sup>-1</sup>, at 25 °C (Table 1: R5T, with the iron content too small to be plotted in Fig. 4(b), and R6T) the iron concentration is also smaller (never larger than 0.15 mg L<sup>-1</sup>) but conversions of 2-CP and TOC are at any rate too low. Still at low catalyst loading, when the temperature is raised to 50 °C and conversions of 2-CP and TOC reach favorable outcomes (Table 1: R8T and Fig. 2(a) and (b)), the iron concentration increases up to 1.4 mg L<sup>-1</sup> shortly before 3 h of reaction. Only after the point where the 2-CP concentration is significantly decreased (approximately right after 3 h of operation) the iron concentration in the solution shows a faster increase reaching a value as high as 4.3 mg L<sup>-1</sup>. This is an important observation considering post-reaction treatment processes. Similarly, but to a much lesser extent, in the case of 2 g L<sup>-1</sup> (Table 1: R3T with Fig. 3(a) and (b)) shows a comparable unfavorable effect, which is, additionally, associated with the fact that most of the sought-after results are unfavorable. The iron concentration reaches lower values (smaller than 0.6 mg L<sup>-1</sup>) that, leaving aside the lack of the demanded reaction efficiency, could have been a very desirable output. Indeed, the interruption of the degradation reaction due to the depletion of the hydrogen peroxide, also affects subsequent steps of the overall reaction. Its absence leads to less significant iron dissolution.

One preliminary conclusion can be reached at this point. The presence of iron in the solution, even in very small amounts is indispensable to start the degradation reaction of 2-CP and concentrations not larger than 2 ppm are enough to reach high 2-CP conversions.

#### 4.4. Iron leaching: evidence of heterogeneous reactions leading to the reaction onset

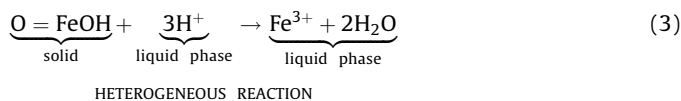
Besides the results shown in Figs. 2 and 3, there are supplementary observations regarding the performance of this reaction. Conversion of 2-CP in Runs R1T, R2T, R5T, R6T, and R10T (see Table 1 and Fig. 4(a) and (b)) show a result that can be interpreted in terms of a rather long time lag for starting a faster decomposition reaction. The induction time described before, is less significant in Runs R3T and R4T and, particularly, in Runs R7T and R8T carried out at higher temperatures. This could be an indication that the time required to build up the required iron concentration in the solution is not the result of an instantaneous process and, at the same time, very much temperature dependent, the latter being again an effect not explored in previous studies.

There are three conceivable processes by which iron can be released into the solution. The first, that is needed to initiate the reaction and most likely responsible for the observed time lags, is the transfer to the solution of the product of a surface proton promoted iron dissolution reaction [41]. The second occurs in the particular case of aryl compounds [49] due to the iron dissolution

activity produced by the existing quinones byproducts. The third is the non-reductive ligand dissolution [50] that can be produced for example by oxalic acid [11]. All of them are typical surface reactions indicating the existence of three additional important heterogeneous reactions. They are subjected to the classical steps of (1) reactant mass transfer, (2) adsorption on the active sites of the iron-contained compounds, (3) surface reaction, (4) desorption and (5) return of reaction products to the bulk of the solution. It should be noted that previous quoted contributions, as well as others mentioned below, were not dealing with water pollution research, but concerned with improving the understanding of iron transformations in soils, sediments and aquifers.

#### 4.4.1. Proton induced dissolution of iron

Let us consider the first possibility. Employing perchloric acid, the mechanism has been shown to be very different from the one with strong acids such as hydrochloric acid [41,51]. At pH 3, the surface of goethite will be surrounded by a high concentration of protons. Goethite is not a dense iron oxide and has double rows of empty octahedral sites [49,52]. This may render the goethite lattice more accessible to the diffusion of chemicals to the inner structure. Thus, it should not be expected to have mass transfer resistances for H<sup>+</sup> (having, in particular, a very large diffusivity) to the active sites of the catalyst. Cornet et al. [41] have proposed a mechanism for the specific attack of perchloric acid to goethite. This suggestion was additionally corroborated by Stumm and Furrer [50,51]. A pictorial representation of the proposal is presented in Fig. 6(a) where it shows the very complex structure of the solid (note that it is very difficult to represent its intervention in a conventional chemical reaction sequence). The authors suggested that the first step involves the formation of a surface Fe<sup>III</sup> atom, coordinated with OH(OH<sub>2</sub>). The Fe<sup>III</sup> atom jointly with the neutral OH(OH<sub>2</sub>) pair absorbs a proton to the OH group of the solid, transforming the surface into a positively charged entity. The equilibrium between the new surface group and the solution is said to be established rapidly. Subsequently, two more protons per Fe<sup>III</sup> atom are absorbed in two separate steps leading to the formation of O = Fe<sup>III</sup>(OH<sub>2</sub>)<sub>2</sub><sup>+</sup> on the surface. This process weakens the Fe<sup>III</sup>–O bond – probably by polarizing it – and thus promotes the detachment of Fe<sup>III</sup> to the interface. This detachment reaction has been described to be slow (it is reported to have a comparatively high activation energy with respect to the others [50]). This reaction is followed by a fast reaction that releases Fe<sup>3+</sup> to the solution. The overall reaction, whose kinetics has been shown to be not affected by the concentration of ClO<sub>4</sub><sup>-</sup> ions, is [41,50]:



On this basis, it is possible to postulate a single mechanistic step for the proton promoted dissolution step to represent the process with the global reaction given by Eq. (3). This result also explains the influential temperature dependence on this iron dissolution

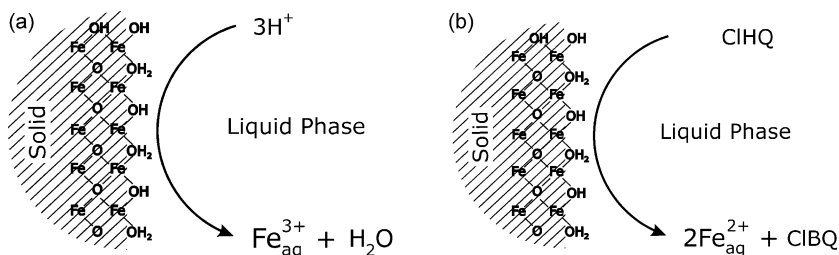


Fig. 6. (a) Pictorial representation of the proton induced iron dissolution. (b) Pictorial representation of the reductive induced iron dissolution.



reaction and confirms the rather high activation energy found for the step represented by the detachment step of  $\text{O} = \text{Fe}^{\text{III}}(\text{OH})_2^+$  [50]. However, mass transfer limitations could lead to the observed slow dissolution process. This problem, will be dealt with, together with other possible mass transport processes existing in this complex, heterogeneous Fenton decomposition of 2-CP, in a specific section below.

#### 4.4.2. 2-CP degradation byproducts reductive dissolution of iron

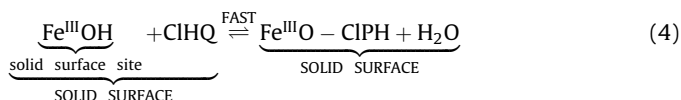
Figs. 2 and 3 also show that at high and low catalyst concentrations, small amounts of reaction intermediates were found and identified as CIBQ and CIHQ. Almost immediately after the moment that these intermediates were detectable, the build up of the iron concentration was accelerated as well as the decomposition rate of 2-CP. Thus, appearance of iron in the reaction solution, for this particular reaction, is also related on the existence of these reaction intermediates. The suggested mechanism of iron transfer into the solution produced by the reductive dissolution on the goethite surface by CIBQ and CIHQ, can be explained and derived from the proposal made by LaKind and Stone [49] for hydroxybenzene reductants, based on previous detailed contributions [44]. These results give rise to the third heterogeneous reaction. The mechanism for this reaction can be illustrated with CIHQ. The same arguments concerning the accessibility of the goethite lattice for the diffusion of chemicals to the inner structure are valid here [49]. Fig. 6(b) is a second pictorial representation of this proposal.

Ref. [49] worked with hydroquinone (HQ). This is a two equivalent reductant of iron oxides(III) [53]. Consequently, it was assumed that CIHQ reacts with 2 mol of goethite of the solid matrix to produce two moles of  $\text{Fe}^{2+}$  plus one mole of benzoquinone (BQ); i.e., two moles of  $\text{Fe}^{\text{III}}$  are reduced for every mole of HQ that is oxidized. For this case the progress of the reaction and the reaction stoichiometry for the pH range from 2 to 8 was studied experimentally by LaKind and Stone [49] (with the majority of the data obtained at pH between 2 and 4), following the concentrations of hydroquinone, benzoquinone and ferrous ion in solution in long term essays. They found that the iron released to the solution was mainly in the form of  $\text{Fe}^{2+}$  (even in the presence of oxygen, as long as the pH was lower than 4) and confirmed empirically the assumed stoichiometry.

To make sure that this reaction can be analyzed in the above mentioned approach, three control experiments were made: (i) the stability of CIBQ and CIHQ at 25 and 50 °C during 6 h; (ii) the interaction of 5 ppm of CIHQ 85% (supplied with 15% of CIBQ) with goethite ( $0.5 \text{ g L}^{-1}$ ) and pH 3 (adjusted with perchloric acid) in a hermetically sealed reactor at 50 °C; (iii) the resulting adsorbed concentration of CIHQ + CIBQ on the catalyst after 6 h (by subtraction from the initial total concentration of both). The following results were obtained: (i) during 6 h, at 25 and 50 °C, CIBQ and CIHQ did not change their initial concentrations; (ii) after 6 h, at 50 °C, in the presence of goethite, most of the CIHQ was transformed into CIBQ (Fig. 10), (iii) under these conditions, and in the absence of 2-CP, a total iron concentration of  $1.5 \text{ mg L}^{-1}$  was released into the solution; (iv) 10% of CIBQ + CIHQ remained adsorbed in the solid. The results indicated in (iii) are in agreement with the same experiment performed by Kung and McBride [53].

Following the ideas described by Refs. [53,49] for hydroxybenzene reductants, the following mechanism, adapted for CIHQ can be tentatively proposed.

Let PH to represent a phenolic ring. The precursor complex-formation reaction is

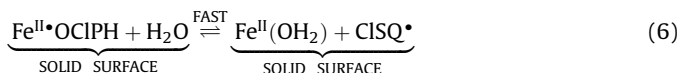


▷ represents a bond to the matrix of the oxihydroxide surface.

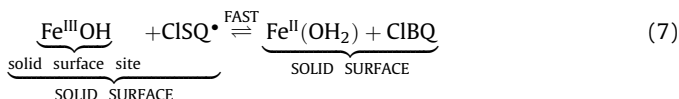
The reaction is followed by an electron transfer:



The unstable reaction intermediate reacts according to:



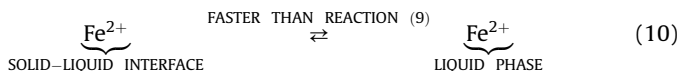
In reaction (6)  $\text{ClSQ}^\bullet$  is the semiquinone radical. Studying the interaction of hydroquinone with iron oxides, Kung and McBride [53] detected, by on-line spectroscopy, the presence of the semiquinone radical, particularly very stable at pH above 6. It can participate in a second oxidation step:



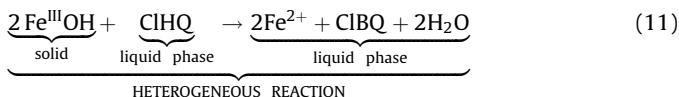
The reduced and positively charged  $\text{Fe}^{2+}$  in reaction (8), is released to the solid-liquid interface:



Finally, from the interface the  $\text{Fe}^{2+}$  is transferred into the bulk of the solution:



The global reaction is:



The net rate of  $\text{Fe}^{2+}$  release is determined by the relative rates of  $\text{Fe}^{2+}$  liberation from the oxide structure to the solution and the  $\text{Fe}^{2+}$  readorption from the overlying solution on the solid. According to [49] the reductive reaction creates an octahedrally located  $\text{Fe}^{\text{II}}$  in the iron oxide structure. Thus, the rate of iron release depends, in part, to the ability of the octahedral site to accommodate the  $\text{Fe}^{\text{II}}$ . If  $\text{Fe}^{\text{II}}$  is too large for the site, the bond breakage will occur more easily and the rate of iron release will increase. A similar effect occurs when  $\text{Fe}^{3+}$  reduces to  $\text{Fe}^{2+}$ . This migration of iron from the solid is a strong function of pH having a maximum efficiency at pH between 3 and 4. Below pH 2 and above pH 6 it is almost a null alternative. Regarding this reductive reaction, the efficiency of CIHQ is exceedingly larger with respect to that of CIBQ [49]. In fact, under these reaction conditions, for goethite, according to [50], this is the most important dissolution mechanisms, much more important than the proton induced dissolution.

The mass transfer process from the interface to the bulk of the solution (reaction (10)) will be analyzed below. In any event, if it is confirmed that effectively reaction (9) is very slow, this result could explain once more the significant influence of temperature in the iron transfer reaction to the liquid phase. This heterogeneous mechanism will be included in the proposed reaction sequence as indicated in reaction (11).

#### 4.4.3. 2-CP degradation byproducts non-reductive dissolution of iron

An important increase in iron concentration in the solution is shown in Figs. 2(b) and 5(b), particularly after the point in which both 2-CP and ClHQ cannot be detected. Besides the proton promoted and quinone reductive dissolution of iron from iron oxides, a third mechanism may be important to explain the observed results. Oxalic acid (OxA) is almost always generated during the oxidation of organic compounds. The combination goethite–H<sub>2</sub>O<sub>2</sub> is not an exception and OxA was positively detected by ion chromatography. The non-reductive dissolution of iron oxides occurs in aqueous oxalic acid solutions and dark surroundings. Following Huang and Huang [11], the non-reductive dissolution pathway of iron oxide is a simple desorption process. The immobilized iron is dissolved by oxalic acid, and a ferric iron complex (Fe<sup>3+</sup><sub>solution</sub>)<sub>complex</sub> is formed. The rate is assumed to be proportional to the driving force existing between the iron in the solid and the one in the solution according to:

$$r_{(\text{Fe}^{\text{III}})_{\text{Solid}}} = -k_{\text{dis.}} [C_{\text{Fe}^{\text{III}}_{\text{Solid}}} - C_{\text{Fe}^{\text{3+}}_{\text{Solution}}}] \quad (12)$$

This process may explain the increase in the dissolved iron concentration after the reaction between the 2-CP and the H<sub>2</sub>O<sub>2</sub> has been stopped either because there is no more hydrogen peroxide or 2-CP or both.

#### 4.4.4. The unusual increase in iron dissolution (R7T and R8T)

An unusual increase in iron concentration is shown in experiments R7T and R8T, particularly after about 4 h of reaction. These results, especially when they are compared with experiments R3T and R4T deserve an explanation. Let us refer to Figs. 2, 3 and 5. The four experiments were made at 50 °C. The only major difference is the catalyst loading: 0.5 g L<sup>-1</sup> for Runs R7T and R8T and 2.0 g L<sup>-1</sup> for Runs R3T and R4T. In the last two cases, the rapid degradation of hydrogen peroxide resulting from the combination of high temperature and high catalyst loading, significantly affects the reaction efficiency. This result does not allow to reaching sufficient concentration of reaction intermediates and, consequently, the reductive dissolution of iron is severely decreased, leading to the lack of enough dissolved iron for an efficient development of the homogeneous Fenton reaction. The consequence is clearly seen when conversions of 2-CP and TOC in these two runs are compared with those corresponding to Runs R7T and R8T. On the contrary, in the last mentioned cases, when the catalyst concentration is lower (at the same high temperature) the reaction is much more efficient and the important contribution of the reductive dissolution by ClHQ occurs. This effect, combined with the subsequent involvement of oxalic acid in the later stages of the reaction (after most of the 2-CP has been degraded) produces a significant increase in the concentration of dissolved iron. These two phenomena are very much minimized in experiments R3T and R4T.

### 5. Mass transfer limitations

There are three processes that deserve examination: (i) the possibility of a diffusion controlled mass transfer of 2-CP inside the pores, (ii) the possibility of the OH• radicals, produced by the hydrogen peroxide decomposition to diffuse from the goethite porous structure into the bulk of the liquid and (iii) the possibility that the liberated Fe(OH)<sup>2+</sup> (in the proton promoted reaction not shown in details in Section 4.4.1), Fe<sup>2+</sup> or Fe<sup>3+</sup> ions (resulting from other dissolution mechanisms) could be mass transfer controlled either inside the pores or at the liquid boundary layer surrounding the catalytic particle.

The first one can be readily analyzed by employing the Weisz–Pratter criteria ( $M_{W-P}$ ) [54,55] that can be calculated from

observable quantities and known information and given by  $C_{W-P} = -r_A'''(\text{Obs.})R_{\text{Part}}^2/D_{\text{Eff.}}C_A^{\text{Surf.}}$ . When  $M_{W-P} \ll 1$  it is unquestionably sure that there are no mass transfer limitations inside the pores and when  $M_{W-P} \gg 1$ , without any doubt mass transfer limitations are surely present. Assuming from the moment that there is no external mass transfer control, all the data in previous equation can be calculated ( $D_{\text{Eff.}} = D_{\text{AB}}^0 \varepsilon_{\text{Solid}} \sigma_{\text{Solid}} / \tau_{\text{Solid}}$ ). The diffusivity can be readily calculated, the porosity is known and safe values for the constriction factor ( $\rho_{\text{Solid}}$ ) and the tortuosity factor ( $\tau_{\text{Solid}}$ ) are 0.8 and 3, respectively.  $r_A'''(\text{Obs.})$  is the maximum observed volumetric reaction rate. The test can be made with one of the substances that have the highest molecular weight. For 2-CP, the effective diffusivity results  $1.78 \times 10^{-6} \text{ cm}^2 \text{ s}^{-1}$ . Then,  $C_{W-P} = 0.0048 \ll 1$ . Consequently, for 2-CP no mass transfer limitations exists inside the catalytic particles.

The same analysis can be repeated for the ability of OH• radicals resulting from the hydrogen peroxide surface decomposition to reach the bulk of the liquid. From the decomposition rate of hydrogen peroxide [3] the decomposition rate constant of hydrogen peroxide decomposition is  $2.1 \times 10^9 \text{ M}^{-1} \text{ s}^{-1}$  [3]. The maximum calculated concentration of OH• with simulation experiments is  $1.5 \times 10^{-11} \text{ M}$  (see companion article by the authors: Ortiz de la Plata et al. [56]). A low scavenger concentration (C<sub>H<sub>2</sub>O<sub>2</sub></sub>) was taken as 10% of the initial concentration. The use of a scavenger instead of direct recombination of radicals will render a more conservative estimation. The effective diffusivity of OH•, larger than that of 2-CP, was estimated to be  $1 \times 10^{-6} \text{ cm}^2 \text{ s}^{-1}$  [3]. All other data were known. The result renders a value of  $C_{W-P} \approx 6.6 \times 10^7 \gg 1$ . Thus, the termination rate is so fast as compared with the mass transfer rate that these radicals will have a very low chance of reaching the bulk of the fluid.

The next problem is to know whether the migration of Fe(OH)<sup>2+</sup> or Fe<sup>2+</sup> or Fe<sup>3+</sup> from the catalyst surface to the bulk of the fluid is controlled by external mass transfer as compared with the reactions occurring on the surface of the catalyst. Let us consider the compound with the larger molecular weight. The mass transfer coefficient must be calculated to compare the mass transport rate with the observed interfacial reaction. The mass transfer coefficient can be calculated with the correlation of Caldelbrank and Moo-Young [57] for small particles. It requires the value of the diffusivity, for example, for Fe(OH)<sup>2+</sup>. The value is known:  $D \approx 5.9 \times 10^{-6} \text{ cm}^2 \text{ s}^{-1}$  [58]. The result for the mass transfer coefficient is  $k_s = 0.007\text{--}0.008 \text{ cm s}^{-1}$  depending on the particle size. The rate cannot be faster than the maximum observed rate of 2-CP degradation. With a pseudo-first order approximation, the rate constant in the “bulk” of the fluid ( $k'''$ ) can be transformed into a surface rate constant ( $k''$ ) dividing by  $S_g \times C_{\text{Cat-Mass}}$ . Both values are known. The maximum observed pseudo-first order constant in the bulk is  $2.7 \times 10^{-4} \text{ s}^{-1}$ . Resorting to the second Damköhler number [59] we obtain  $\text{Da}^{\text{II}} = k''_{\text{Surface}}^{\text{Obs.}} / k_s = 0.54 \times 10^{-4}$ . Thus, taken into account the low value of  $\text{Da}^{\text{II}}$ , the iron dissolution rate (the interfacial reaction) is very slow as compared with the mass transport rate. Consequently, this is a confirmation that the heterogeneous surface reaction is in all cases the rate-controlling step. This calculation also ratifies the one made in Ref. [2] concerning the competition of the HO• recombination rate with respect to their mass transfer rates to the bulk of the solution.

Thus, it can be concluded that in the three cases, there is a heterogeneous, goethite surface rate-controlling step. It is very important to remark once more that once very low concentrations of Fe<sup>2+</sup> in the solution are established, they are sufficient to carry out the reaction and produce these intermediates needed for the third heterogeneous process. The steep ramp in iron concentration in the solution, produced when the reductive dissolution by chloroquinones reaches its maximum activity could be avoided

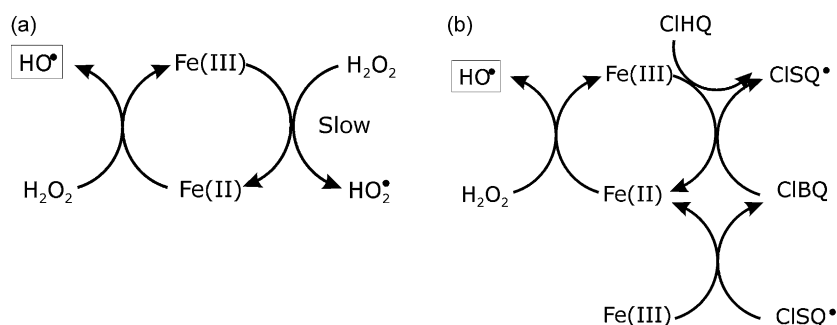


**Fig. 7.** (a) Schematic representation of the  $\text{Fe}^{3+} \leftrightarrow \text{Fe}^{2+}$  cycle in the Fenton reaction. (b) Schematic representation of the reaction enhancement produced by ClHQ. Formats adapted from [42].

after 3 h of reaction (a 2-CP conversion close to 98%) and the process combined with other AOTs for complete mineralization. In spite of it, it is clear that the presence of one or both heterogeneous reactions in parallel is necessary condition for the onset of the Fenton reaction at pH 3.

## 6. The general mechanism of the homogeneous–heterogeneous Fenton reaction

### 6.1. Classical homogeneous Fenton reaction

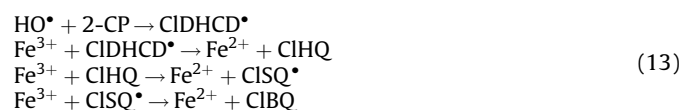
Up to this point it has been shown the significance of four heterogeneous reactions: (I) to explain the unusually high consumption of hydrogen peroxide, (II) to explain the proton dissolution of iron, (III) to elucidate the reductive dissolution of iron and (IV) to rationalize the unusual increase in the rate of iron dissolution after most of 2-CP and hydrogen peroxide have been decomposed. In addition, we will further discuss the homogeneous reactions that lead to the intensification of the  $\text{Fe}^{3+} \rightarrow \text{Fe}^{2+}$  transformation. It has also been commented before that once processes (II) and (III) have taken place, the 2-CP degradation transforms into a particular case of a homogeneous Fenton reaction. Hence, there is no need to repeat the details of a part of the process that is already known. It is possible to resort to the many proposals existing in the literature [33,42,60] just to mention some relevant reports. In this work, it has been chosen the classical approach, as compared with the non-classical Fenton pathways based in the formation of high valent oxoiron complexes [33]. The

formation of hydroxyl radicals and the mechanism of the cyclical transformation of  $\text{Fe}^{3+} \rightleftharpoons \text{Fe}^{2+}$ , without the intervention of 2-CP byproducts, have been described through several well-known reactions (see schematic representation in Fig. 7(a) with a format adopted from Ref. [42]). They have been included in Table 2 as reaction steps 2–8.

### 6.2. Homogeneous enhancement of the reaction rate by 2-CP degradation byproducts

It has been originally reported by Lu [19], without exact chemical identification that some reductive compounds existing in the reacting mixture causes the incorporation of iron into the solution. These authors also reported that, when these compounds act, they substitute the iron proton dissolution as the new rate-controlling step for the complete oxidation of 2-CP. This statement has been confirmed in this work with experimental evidence, because no concentrations of reaction intermediates were measured in previous reports.

Furthermore, this is not the only important effect of these byproducts. Other reactions produced by 2-CP degradation in the homogeneous phase, play a very significant role in an enhancement of the transformation of  $\text{Fe}^{3+}$  to  $\text{Fe}^{2+}$  according to the following scheme proposed and validated for phenol by Chen and Pignatello [42,61] and modified here for 2-CP (see Fig. 7(b) adapted from the quoted reference):



In the reactions included in (13), ClDHCD• is the chlorodihydroxycyclohexadienyl radical and ClSQ• is the chlorosemiquinone radical. Thus according to reactions (13) the presence of quinone byproducts not only induces the iron reductive dissolution, but also they are major contributors to the restoring of the  $\text{Fe}^{2+}$  species, improving what is recognized as a relatively slow step in the classical Fenton reaction. The second reaction in the set of reactions (13) also contributes to the formation of ClHQ, which is also very important to the incorporation of iron into the homogeneous phase, as discussed before.

To confirm the function carried out by quinone byproducts in this reaction, two additional runs were made to parallel the results obtained in Run R8T (Table 1) with experiments made adding, separately, an initial concentration of 5% (w/w) of ClBQ or ClHQ. Results for the second case are shown in Fig. 8 (R14T). The two effects: (i) participation in the surface reaction and (ii) contribution in the homogeneous reaction cannot be separated with these experiments. In any event, in the case of ClHQ the following beneficial results are shown after 3 h of reaction: (1) The time lag for the initiation of reaction is further reduced. (2) As a main

**Table 2**  
Proposed reaction scheme.

No. 1	$\text{FeOOH} + 3\text{H}^+ \rightarrow \text{Fe}^{3+} + 2\text{H}_2\text{O}$	[41]
No. 2	$\text{Fe}^{3+} + \text{H}_2\text{O}_2 \rightarrow \text{Fe}^{2+} + \text{H}^+ + \text{HO}_2^\bullet$	[33,42]
No. 3	$\text{Fe}^{2+} + \text{H}_2\text{O}_2 \rightarrow \text{Fe}^{3+} + \text{HO}^\bullet + \text{HO}^\bullet$	[33,42]
No. 4	$\text{H}_2\text{O}_2 + \text{HO}^\bullet \rightarrow \text{HO}_2^\bullet + \text{H}_2\text{O}$	[33,42]
No. 5	$\text{H}_2\text{O}_2 + \text{HO}_2^\bullet \rightarrow \text{HO}^\bullet + \text{H}_2\text{O} + \text{O}_2$	[33,42]
No. 6	$\text{Fe}^{3+} + \text{HO}_2^\bullet \rightarrow \text{Fe}^{2+} + \text{H}^+ + \text{O}_2$	[33,42]
No. 7	$\text{Fe}^{2+} + \text{HO}_2^\bullet + \text{H}^+ \rightarrow \text{Fe}^{3+} + \text{H}_2\text{O}_2$	[33,42]
No. 8	$\text{Fe}^{2+} + \text{HO}^\bullet \rightarrow \text{Fe}^{3+} + \text{HO}^\bullet$	[33,42]
No. 9	$\text{HO}^\bullet + 2\text{-CP} \rightarrow \text{ClDHCD}^\bullet$	[33,42]
No. 10	$\text{Fe}^{3+} + \text{ClDHCD}^\bullet \rightarrow \text{Fe}^{2+} + \text{ClHQ}$	[42,60]
No. 11	$2\{\text{FeOH}\} + \text{ClHQ} \rightleftharpoons 2\text{Fe}^{2+} + \text{ClBQ} + 2\text{H}_2\text{O}$	[49,50] <sup>a</sup>
No. 12	$\text{Fe}^{3+} + \text{ClHQ} \rightarrow \text{Fe}^{2+} + \text{ClSQ}^\bullet$	[42,60]
No. 13	$\text{Fe}^{3+} + \text{ClSQ}^\bullet \rightarrow \text{Fe}^{2+} + \text{ClBQ}$	[42,60]
No. 14	$\text{ClDHCD}^\bullet + \text{O}_2 \rightarrow \text{ClHQ} + \text{HO}_2^\bullet$	[42,62]
No. 15	$\text{ClDHCD}^\bullet + \text{O}_2 \rightarrow \text{Products}$	[42,62]
No. 16	$\text{HO}^\bullet + \text{ClBQ} \rightarrow \text{Products}$	[42,60]
No. 17	$\text{HO}^\bullet + \text{ClDHCD}^\bullet \rightarrow \text{Products}$	[42,60]
No. 18	$\text{HO}^\bullet + \text{ClHQ} \rightarrow \text{Products}$	[42,60]
No. 19	$\text{H}_2\text{O}_2 \xrightarrow{\text{FeOOH}} \frac{1}{2}\text{O}_2 + \text{H}_2\text{O}$	[2,3]

2-CP: 2-chlorophenol; ClDHCD•: chlorodihydroxycyclohexadienyl radical; ClHQ: chlorohydroquinone; ClBQ: chlorobenzoquinone; ClSQ•: chlorosemiquinone radical; FeOOH: solid goethite.

<sup>a</sup> Adapted.

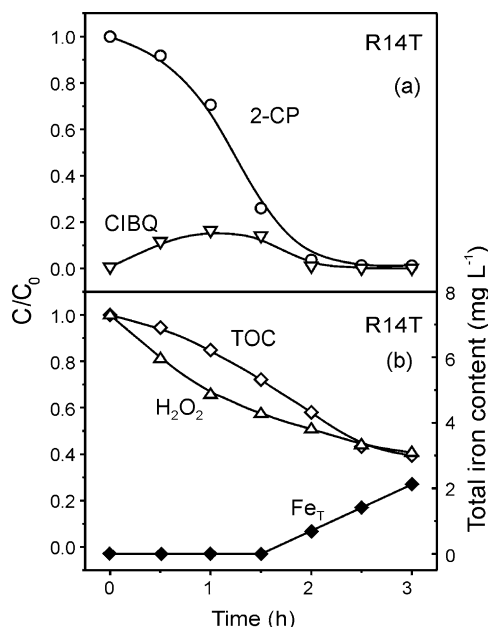


**Fig. 8.** Dimensionless concentrations of reactants and products versus time. 5% addition of ClHQ. R14T:  $C_{\text{Cat}} = 0.5 \text{ g L}^{-1}$ ,  $R = 50$  and  $T = 50^\circ \text{C}$ . (a)  $\circ$ ,  $C_{2\text{-CP}}/C_{2\text{-CP},0}$ ;  $\nabla$ ,  $C_{\text{CIBQ}}/C_{2\text{-CP},0}$ . (b)  $\diamond$ ,  $\text{TOC}/\text{TOC}_0$ ;  $\triangle$ ,  $C_{\text{H}_2\text{O}_2}/C_{\text{H}_2\text{O}_2,0}$ ;  $\blacklozenge$ , total dissolved iron.

consequence of the shorter reaction time (3 h vs. 6 h), consumption of H<sub>2</sub>O<sub>2</sub> has been reduced from 86% to 59%. (3) Conversion of 2-CP is almost 100%. (4) The iron content reaches a value of  $2.1 \text{ mg L}^{-1}$  (with a value of  $1.5 \text{ mg L}^{-1}$  when 2-CP conversion is 98% after 3 h of reaction). Finally, (5) an undesired consequence of the reduction in the reaction time, causes that some of the byproducts do not reach the same degree of mineralization and the TOC conversion is only 60%. However, in Run R8T, after 3 h of reaction, the TOC concentration was approximately 56%. Experiments with CIBQ produced similar results (R15T in Table 1).

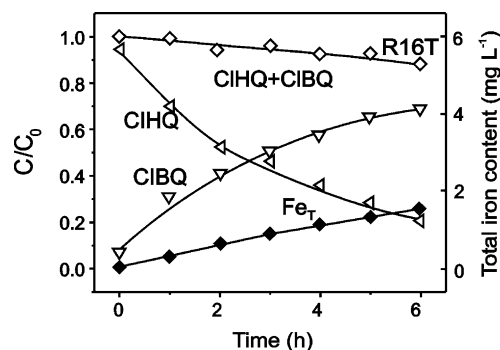


**Fig. 10.** Dimensionless concentrations of reactants and products versus time. 5 ppm initial concentration of ClHQ. R16T:  $C_{\text{Cat}} = 0.5 \text{ g L}^{-1}$  and  $T = 50^\circ \text{C}$ .  $\diamond$ ,  $(C_{\text{ClHQ}} + C_{\text{CIBQ}})/(C_{\text{ClHQ},0} + C_{\text{CIBQ},0})$ ;  $\triangleleft$ ,  $C_{\text{ClHQ}}/(C_{\text{ClHQ},0} + C_{\text{CIBQ},0})$ ;  $\nabla$ ,  $C_{\text{CIBQ}}/(C_{\text{ClHQ},0} + C_{\text{CIBQ},0})$ ;  $\blacklozenge$ , total dissolved iron.

### 6.3. Proposal of a feasible reaction scheme

After the discussions presented in the previous sections, it is possible to propose a feasible reaction scheme for the studied reaction considering that it progresses with a combined mechanism of heterogeneous and homogeneous reactions. This action, leads to the onset of the homogeneous Fenton process, which is produced when a small concentration of iron leaches into the homogeneous solution. It is schematically presented in Fig. 9 with the details depicted in Table 2. The reactions mentioned explicitly in Fig. 9 are the ones shaded in Table 2.

This proposal of a workable reaction mechanism must be complemented with the specific steps of the four surface reactions. They should be very useful for two additional intended applications: (i) to develop mechanistically based reaction kinetics for the heterogeneous Fenton reaction carried out under the operating conditions of this work and (ii) the extension of this reaction scheme to the heterogeneous photo-Fenton reaction. This sequel has two specific purposes: (a) to increase the reaction efficiency and (b) to be able to carry out the reaction employing solar radiation. The use of this technology, not only provides radiation for the photo-activated process, but also the heating of the reacting mixture up to  $50^\circ \text{C}$  (the best observed operating condition using low catalyst concentration) with no additional costs of energy.

## 7. Conclusions

A detailed description of a heterogeneous-homogeneous Fenton reaction mechanism applied to the decomposition of 2-CP, employing particulate goethite at pH  $3 \pm 0.1$  has been proposed and supported with experiments.

The reaction is based on the incorporation of iron into the solution by two different mechanisms: (i) a interfacial proton dissolution attack reaction on the goethite surface, to start the Fenton homogeneous reaction after the iron compound has been transferred into the solution and (ii) a surface reductive liberation of iron by the reaction byproducts resulting from the degradation of 2-CP (CIBQ and ClHQ) that were detected as reaction intermediates. A third heterogeneous reaction that becomes important when most of 2-CP and H<sub>2</sub>O<sub>2</sub> have been decomposed is produced by a third important reaction byproduct. The existence of a significant increase in the rate of iron dissolution under some particular operating conditions coincides with the detection of oxalic acid in the solution. This compound produces non-reductive iron dissolution.

Once small amounts of iron leach into the solution, the subsequent mechanism is a particular case of a homogeneous Fenton reaction. Iron leaching into the solution is very small, but enough to promote this homogeneous reaction.

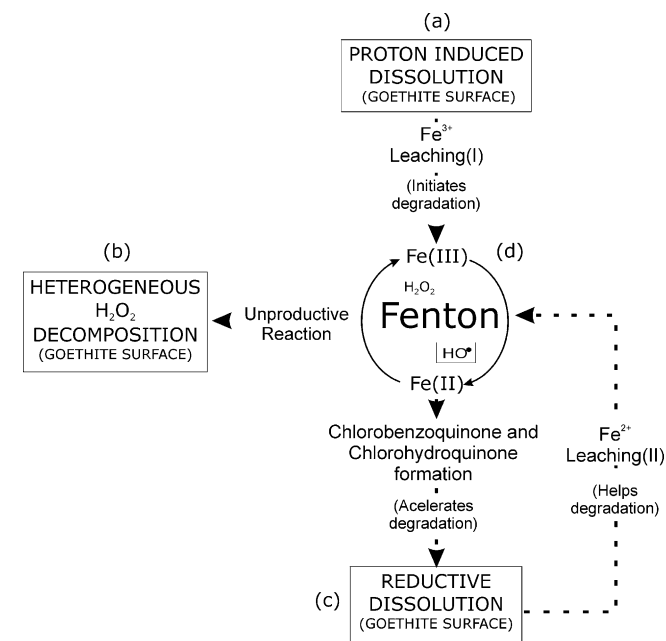


**Fig. 9.** Representative diagram of the combined scheme of heterogeneous and homogeneous reactions participation in the heterogeneous Fenton reaction of 2-CP degradation.



A homogeneous reaction enhancement resulting from reaction byproducts of the 2-CP degradation significantly improves the regeneration of  $\text{Fe}^{2+}$  species. Additional control experiments suggest that this mechanism could be, at least, as important as those heterogeneous reactions that leads to the iron dissolution.

The unusual decomposition of hydrogen peroxide, that is very important, has been explained by the existence of an additional heterogeneous step that seems to have a direct relationship with the existing solid concentration (particularly with rather large surface area) and temperature.

A catalyst concentration of  $0.5 \text{ g L}^{-1}$ , a molar ratio of  $\text{H}_2\text{O}_2$  to 2-CP between 30 and 50 and a temperature of  $50^\circ\text{C}$  were found to be the best operating conditions within the range of the explored variables.

## Acknowledgements

The authors would like to thank to Universidad Nacional del Litoral, Consejo Nacional de Investigaciones Científicas y Técnicas and Agencia Nacional de Promoción Científica y Tecnológica for their financial support. The authors gratefully thank Ms. Susana Gervasio for the AAS analysis of the iron samples. Thanks are also given to Professor Miguel Baltanás for his valuable suggestions concerning adsorption experiments and Spectroscopic Analyses. The technical assistance of Eng. Claudia Romani is also acknowledged.

## References

- [1] H.J.H. Fenton, *J. Chem. Soc., Dalton Trans.* 65 (1894) 899–911.
- [2] S.-S. Lin, Interaction of  $\text{H}_2\text{O}_2(2)$  with Iron Oxide for Oxidation of Organic Compounds in Water, Drexel University, 1997.
- [3] S.S. Lin, M.D. Gurol, *Environ. Sci. Technol.* 32 (1998) 1417–1423.
- [4] J. Fernandez, J. Bandara, A. Lopez, P. Albers, J. Kiwi, *Chem. Commun.* (1998) 1493–1494.
- [5] S.S. Lin, M.D. Gurol, *Water Sci. Technol.* 34 (9 pt 5) (1996) 57–64.
- [6] J. Feng, X. Hu, P.L. Yue, *Environ. Sci. Technol.* 38 (2004) 5773–5778.
- [7] G.B. Ortiz de la Plata, O.M. Alfano, A.E. Cassano, *Chem. Eng. J.* 137 (2008) 396–410.
- [8] J. Fernandez, M.R. Dhananjeyan, J. Kiwi, Y. Senuma, J. Hilborn, *J. Phys. Chem. B* 104 (2000) 5298–5301.
- [9] A. Bozzi, T. Yuranova, J. Mielczarski, A. Lopez, J. Kiwi, *Chem. Commun.* (2002) 2202–2203.
- [10] A. Bozzi, T. Yuranova, J. Mielczarski, J. Kiwi, *New J. Chem.* 28 (2004) 519–526.
- [11] C.P. Huang, Y.H. Huang, *Appl. Catal. A: Gen.* 346 (2008) 140–148.
- [12] M. Neamtu, C. Zaharia, C. Catrinescu, A. Yediler, M. Macoveanu, A. Kettrup, *Appl. Catal. B: Environ.* 48 (2004) 287–294.
- [13] Z.W. Zheng, L.C. Lei, S.J. Xu, P.L. Cen, *J. Zhejiang Univ.: Sci. B* (2004) 206–211.
- [14] J. Feng, X. Hu, P.L. Yue, *Water Res.* 39 (2005) 89–96.
- [15] A. Cuzzola, M. Bernini, P. Salvadori, *Appl. Catal. B: Environ.* 36 (2002) 231–237.
- [16] F. Martínez, G. Calleja, J.A. Melero, R. Molina, *Appl. Catal. B: Environ.* 60 (2005) 181–190.
- [17] F. Martínez, G. Calleja, J.A. Melero, R. Molina, *Appl. Catal. B: Environ.* 70 (2007) 452–460.
- [18] T. Yuranova, O. Enea, E. Mielczarski, J. Mielczarski, P. Albers, J. Kiwi, *Appl. Catal. B: Environ.* 49 (2004) 39–50.
- [19] M.C. Lu, *Chemosphere* 40 (2000) 125–130.
- [20] M.D. Gurol, S.S. Lin, *Water Sci. Technol.* 1 (2001) 131–138.
- [21] H.H. Huang, M.C. Lu, J.N. Chen, *Water Res.* 35 (2001) 2291–2299.
- [22] S. Chou, C. Huang, Y.H. Huang, *Environ. Sci. Technol.* 35 (2001) 1247–1251.
- [23] Y.T. Lin, M.C. Lu, *Water Sci. Technol.* 55 (12) (2007) 101–106.
- [24] M.C. Lu, J.N. Chen, H.H. Huang, *Chemosphere* 46 (2002) 131–136.
- [25] R. Andreozzi, V. Caprio, R. Marotta, *Water Res.* 36 (2002) 2761–2768.
- [26] R. Andreozzi, A. D'Apuzzo, R. Marotta, *Water Res.* 36 (2002) 4691–4698.
- [27] S. Lee, J. Oh, Y. Park, *Bull. Korean Chem. Soc.* 27 (2006) 489–494.
- [28] D.Q. Wu, G.Y. Diao, P. Yuan, *Br. Mineral. Petrol. Geochim.* 25 (2006) 293–298.
- [29] R. Matta, K. Hanna, S. Chiron, *Sci. Total Environ.* 385 (2007) 242–251.
- [30] A.L. Teel, C.R. Warberg, D.A. Atkinson, R.J. Watts, *Water Res.* 35 (2001) 977–984.
- [31] J. Bandara, U. Klehm, J. Kiwi, *Appl. Catal. B: Environ.* 76 (2007) 73–81.
- [32] M. Cheng, W. Song, W. Ma, C. Chen, J. Zhao, J. Lin, H. Zhu, *Appl. Catal. B: Environ.* 77 (2008) 355–363.
- [33] J.J. Pignatello, E. Oliveros, A. MacKay, *Crit. Rev. Environ. Sci. Technol.* 36 (2006) 1–84.
- [34] O.M. Alfano, R.J. Brandi, A.E. Cassano, *Chem. Eng. J.* 82 (2001) 209–218.
- [35] C.S. Zalazar, M.D. Labas, R.J. Brandi, A.E. Cassano, *Chemosphere* 66 (2007) 808–815.
- [36] C.S. Zalazar, M.E. Lovato, M.D. Labas, R.J. Brandi, A.E. Cassano, *Chem. Eng. Sci.* 62 (2007) 5840–5853.
- [37] H. Gallard, J. De Laat, *Water Res.* 34 (2000) 3107–3116.
- [38] A. Burbano, D. Dionysiou, M. Suidan, T. Richardson, *Water Sci. Technol.* 47 (2003) 165–171.
- [39] G. Sagawe, A. Lehnard, M. Lubber, D. Bahnemann, *Helv. Chim. Acta* 84 (2001) 3742–3759.
- [40] J. Farias, G.H. Rossetti, E.D. Albizzati, O.M. Alfano, *Ind. Eng. Chem. Res.* 46 (2007) 7580–7586.
- [41] R.M. Cornell, A.M. Posner, J.P. Quirk, *J. Inorg. Nucl. Chem.* 38 (1976) 563–567.
- [42] R. Chen, J.J. Pignatello, *Environ. Sci. Technol.* 31 (1997) 2399–2406.
- [43] T.R. Gordon, A.L. Marsh, *Catal. Lett.* 132 (2009) 349–354.
- [44] W.M. Stumm (Ed.), *James Aquatic Chemistry: Chemical Equilibria and Rates in Natural Waters*, 3d ed., John Wiley, New York, 1995.
- [45] W.P. Kwan, B.M. Voelker, *Environ. Sci. Technol.* 38 (2004) 3425–3431.
- [46] W.P. Kwan, B.M. Voelker, *Environ. Sci. Technol.* 37 (2003) 1150–1158.
- [47] A.L. Teel, D.D. Finn, J.T. Schmidt, L.M. Cutler, R.J. Watts, *J. Environ. Eng.* 133 (2007) 853–858.
- [48] J.J. Pignatello, *Environ. Sci. Technol.* 26 (1992) 944–951.
- [49] J.S. LaKind, A.T. Stone, *Geochim. Cosmochim. Acta* 53 (1989) 961–971.
- [50] R.M. Cornell, U. Schwertmann, *The Iron Oxides: Structure, Properties, Reactions, Occurrences and Uses*, Wiley VCH, Weinheim, 2003.
- [51] W. Stumm, G. Furrer, *Aquatic Surface Chemistry*, Wiley and Sons, 1987.
- [52] C.S.J. Hurlbut, C. Klein, *Manual of Mineralogy*, Wiley and Sons, New York, 1977.
- [53] K.H. Kung, M.B. McBride, *Clays Clay Miner.* 36 (1988) 303–309.
- [54] H.S. Fogler (Ed.), *Elements of Chemical Reaction Engineering*, 3d ed., Prentice Hall, New Jersey, 1999.
- [55] O. Levenspiel, *The Chemical Reactor Omnibook*, OSU Book Stores, Corvallis, OR, 1993.
- [56] G.B. Ortiz de la Plata, O.M. Alfano, A.E. Cassano, *Appl. Catal. B: Environ.* 95 (2010) 14–25.
- [57] P.H. Calderbank, M.B. Moo-Young, *Chem. Eng. Sci.* 16 (1961) 39–54.
- [58] A.F. Gil, L. Galicia, I. Gonzales, *J. Electroanal. Chem.* 417 (1996) 129–134.
- [59] R.B. Bird, W.E. Stewart, E.N. Lightfoot (Eds.), *Transport Phenomena*, 2nd ed., J. Wiley, New York, 2002.
- [60] N. Kang, D.S. Lee, J. Yoon, *Chemosphere* 47 (2002) 915–924.
- [61] R. Chen, J.J. Pignatello, *J. AOT* 4 (1999) 447–453.
- [62] J. Ma, W. Song, C. Chen, M. Cheng, W. Ma, J. Zhao, Y. Tang, *Environ. Sci. Technol.* 39 (2005) 5810–5815.